

Effects of Introducing 2-aminoethanethiol into 4-pyridineethanethiol Self-assembled Monolayer Applicable to Enhance Sensitivity of Hg(II) Electrochemical Analysis

P.H. Phong, D.T. Huyen, N.H. Anh and V.T.T. Ha

Institute of Chemistry, Viet Nam Academy of Science and Technology, 18- Hoang Quoc Viet Road, Cau Giay District, Ha Noi, Viet Nam

Received: June 12, 2015, Accepted: October 01, 2015, Available online: October 28, 2015

Abstract: In our work, enhancement of sensitivity of Hg(II) determination by introducing 2-aminoethanethiol (AET) from solutions into the self-assembled monolayers (SAMs) of 4-pyridineethanethiol (PET) on gold nanoparticles (Au-NPs) capped on glassy carbon electrode was studied. The formation of binary SAMs was indicated by the shift of reductive desorption peak to negative potentials in voltammograms recorded in 0.5 M KOH solution. Effects of introduction AET were monitored by FTIR that there was a rapid increase of intensities at bands of 1296 and 1189 cm^{-1} ascribed to (C-H)_{ring} deformation and (C-N)_{ring} stretching, respectively, with increasing immersion time. However, these bands became lower with prolonging more time as well as increasing the concentration of AET in solution. These effects were interpreted due to the conformation of pyridine ring and formation of intermolecular hydrogen bonding between PET and AET. The differential pulse voltammetry for reoxidation of Hg(0) showed the increase of peak current induced by the first effect, whereas the later caused the decrease. Since the optimized conditions, the detection limit for the binary SAMs could approach to 3.85×10^{-12} M Hg(II), approximately three times lower than that of PET SAM.

Keywords: binary SAMs, 4-pyridineethanethiol (PET), 2-aminoethanethiol (AET).

1. INTRODUCTION

Chemisorbed organosulfur self-assembled monolayers (SAMs) have become attractive to many studies in the field of analytical electrochemistry because this type of materials can be pre-designed to introduce specific interactions between the monolayer and analytes [1-3]. Thus, the electrodes modified with SAMs can be tuned in term of sensitivity, selectivity and reproducibility in a relatively short time frame [4-6]. Since such prominent properties, SAMs have been widely used to modify electrodes for electrochemical analysis of heavy metal ions due to their severely harm human health at very low concentrations. Those numerous studies have been briefly reported in literatures [7-10].

Though, the termini of SAM molecules are often composed of only one type of functional group, the chelation specificity is insufficient. Therefore, a way to improve effectiveness is to introduce multifunctional terminal groups so that the chelation discrimination between the interfering substances and analytes is enhanced. Many techniques have been employed to modify the electrode surface for the purpose of determination of heavy metal ions,

such as chemical attachment of peptides on SAMs [11,12], formation of covalent or non-covalent bonds between the template molecules and functional monomers [13-15], molecular imprinting on SAMs [16], formation of multilayer assemblies containing heavy metal ions [17], preparation of the gold interface in micro-/nanopore arrays containing thiol compound [18] or in microporous and mesoporous scale [19], coadsorption of mixed functionalized SAMs [20], adsorption of two components through separated steps [21,22]. As a simple manner, use of multi-components to tailor the surface properties of SAMs can be more advantageous over the single component in specific analysis. There have been, however, relatively few studies of heavy metal determination by electrodes modified with mixed SAMs. For instant, a mixture of 3-mercaptopropionic acid and glutathione enhances the selectivity and sensitivity for Cu(II) analysis compared to the single glutathione SAM modified gold electrode [21].

The present work was prompted by our previous discovery that PET SAM functionalized Au-NPs on glassy carbon electrode (GCE) can be employed for detection of Hg(II) [23]. Hence, the purpose of this study is to further improve the advantage of this type of SAM-modified electrode in determination of Hg(II) at ultra

*To whom correspondence should be addressed: Email: phphong@ich.vast.vn
Phone: 84 4 38362008

concentrations. Herein, we demonstrate a way to enhance the sensitivity of Hg(II) detection by introducing AET from solution into the original PET SAM to form binary SAMs. PET is employed because it can incorporate with Hg(II) at N-pyridine terminal. Besides π - π interaction between lateral pyridine rings that can stabilize PET SAM, its short alkyl chain can also increase electron transfer compared with alkanethiols having longer chains [24,25]. Meanwhile, AET, having similar alkyl chain length is expected to adsorb on vacant sites between lateral PET molecules on Au-NPs to enhance the stability of PET-AET SAMs. In addition, NH_2 terminal group can also incorporate with Hg(II) due to Lewis base-acid mechanism. The binary SAMs, thus, has more capability in incorporating with Hg(II). Furthermore, effects induced by introducing AET into PET SAM affect the sensitivity of Hg(II) detection is also studied by FTIR to provide a closer look on the formation of the binary SAMs.

2. EXPERIMENTALS

2.1. Reagents

4-pyridineethanethiol hydrochloride (PET), 2-aminoethanethiol (AET) purchased from Wako Chemicals was used without further purification. $\text{Hg}(\text{NO}_3)_2$ stock solution (5.0×10^{-3} M) purchased from Merck was used for dilution. More diluted solutions were prepared daily from the stock solution. All other reagent grade chemicals were used without further purification.

2.2. Apparatus

Electrochemical measurements were performed with a home-made potentiostat/galvanostat. A three-electrode configuration was used for measurements, which consists of modified GCE working electrode, calomel (saturated) reference electrode and Pt counter electrode.

Scanning electron microscopy (SEM) images were obtained with a Hitachi S-4800 instrument at acceleration voltage of 15 - 20 kV and a working distance of 4-5 mm.

FTIR measurement was recorded at atmospheric pressure with a FTIR-6300 spectrometer with a liquid-nitrogen cooled narrow band data recorded with a resolution of 4 cm^{-1} using p-polarized radiation at an incidence angle of 45° relative to the surface normal.

2.3. Pretreatment of GCE

The GCE was prepared by cutting available plate-shaped glassy carbon (Tokai GC-20 company, NY) into cylinder-shape and mounting into teflon tubes holder so that only a circular area of 0.071 cm^2 (roughness factor, $\rho = 1.2$) was exposed to the electrolyte. Electrochemical pretreatment of GCE used for further modification was described in elsewhere [23].

2.4. Preparation of Au-NPs

Electrochemical deposition of Au-NPs on the GCE (Au-NPs/GCE) surface was carried out at potential of +0.5 V in 1.0×10^{-3} M HAuCl_4 solution for 600 seconds under stirring rate of 50 rpm. The obtained surface of Au-NPs was used for preparation of SAMs as shown in inset of Figure 1.

2.5. Preparation of PET SAM, AET SAM, and binary SAMs of PET-AET

The single SAMs of PET and AET were prepared by immersing

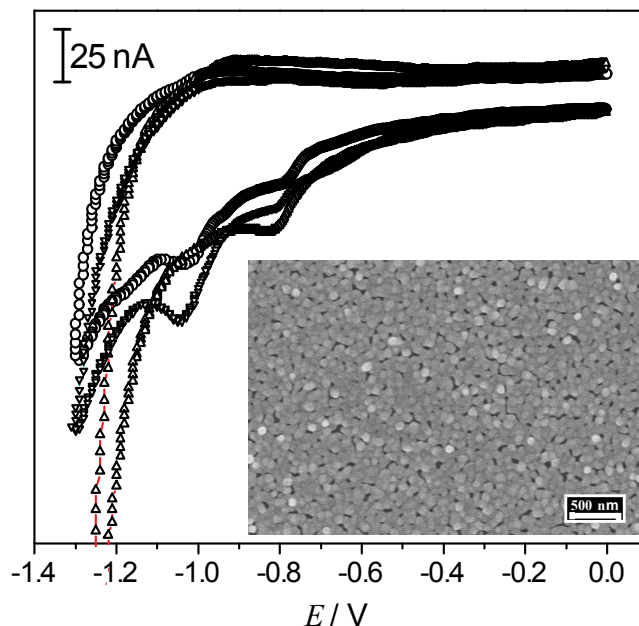


Figure 1. Cyclic voltammograms for reductive desorption of SAMs of PET (\circ), AET (Δ), and PET-AET (∇) prepared by immersing PET SAM into 1.0×10^{-4} M solution of AET for 10 min., recorded in 0.5 M KOH solution, $\nu = 0.1$ V/s. Inset: SEM of Au-NPs/GCE employed for all measurements in the present works.

Au-NPs/GCE into 1.0×10^{-6} M ethanolic solution of PET and AET, respectively, over night at room temperature.

Binary SAMs composed of PET and AET (PET-AET SAMs) was prepared by immersing the original PET SAM into ethanolic solution of AET with various concentrations for duration from 1 to 60 minutes to study relative effects.

2.6. Electrochemical measurements

The characteristics of SAMs functionalized Au-NPs/GCE was investigated by cyclic voltammetry (CV) for reductive desorption. Measurement was performed in 0.5 M KOH solution, from 0.0 V to -1.2 V at scan rate of $0.1 \text{ V} \cdot \text{s}^{-1}$.

Detection of Hg(II) was achieved with following steps. First, Hg(II) was pre-concentrated on SAMs/Au-NPs/GCE in a 0.1 M KCl + HCl solution, pH 6.7 under open circuit potential, stirring at 60 rpm. Next, desorption cathodic potential at -0.6 V was applied in 0.1 M KCl + HCl solution, pH 3.0 for 60 s to reduce Hg(II) to Hg(0). Finally, the differential pulse voltammetry (DPV) was employed to measure the reoxidation peak current of Hg(0) (i_{Hg0}) with the potential was scanned from +0.3 V to +0.7 V; pulse amplitude 0.050 V; pulse time 0.040 s; voltage step 0.005 V; step time 0.08 s; sweep rate $0.05 \text{ V} \cdot \text{s}^{-1}$.

All measurements were performed at room temperature.

3. RESULTS AND DISCUSSION

The macroscopic characteristics of SAMs of PET, AET and binary PET-AET SAMs on Au-NPs/GCE studied by electrochemically reductive desorption technique are shown in Fig. 1, as described in literatures [26,27]. Only a reduction peak of AET-SAM

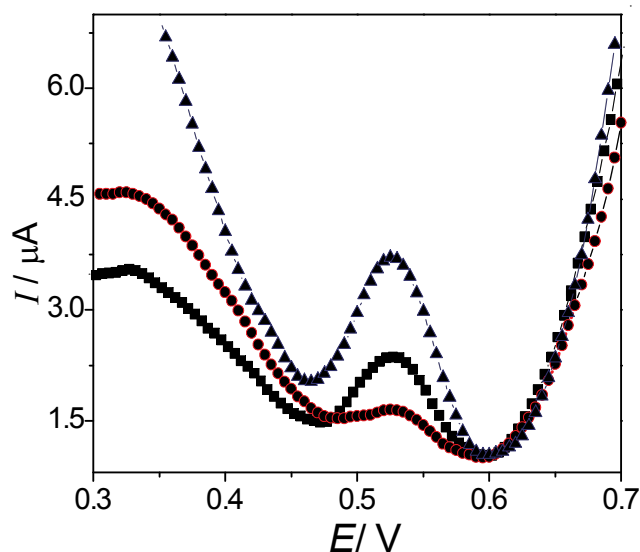


Figure 2. DPV for reoxidation of Hg(0) preconcentrated from 0.1 M KCl + HCl solution containing 4.97×10^{-9} M Hg(II), pH 6.7 on SAMs of AET (●), PET (■), and PET-AET (▲), recorded in 0.1 M KCl + HCl solution, pH 3.0 solution.

appears at potential, $E = -0.80$ V. Since the area under the peak, the charge was estimated to be $62.8 \mu\text{C}\cdot\text{cm}^{-2}$. In the case of PET-SAM, the voltammogram shows a peak at $E = -1.02$ V with the charge of $75.3 \mu\text{C}\cdot\text{cm}^{-2}$. These obtained values of charge suggest the formation of full surface coverage of monolayers on Au(111) [28]. Our previous results revealed that Au-NPs prepared under the experimental conditions are mainly Au(111) terrace having diameter of around 70 - 80 nm as typically shown in inset [23]. In addition, on the voltammogram recorded for PET-SAM, a hump also appears at potential of -0.78 V, corresponding with weak lateral interactions of PET molecules in clusters [27]. When AET is introduced into the original PET-SAM from solution, the reductive desorption voltammogram of PET-AET SAM is almost similar with that of PET-SAM, except a slightly shift of the peak around 23 mV to the negative direction. This evidence indicates that binary SAMs is more stable due to not only $\pi - \pi$ interaction between pyridine rings [29], but also the increase of van der Waals interactions between lateral alkyl chains of PET and AET molecules.

The advantage of PET-AET SAMs in improving the sensitivity of Hg(II) detection is demonstrated by the term of peak current as shown in Fig. 2, in which typical voltammograms were recorded by employing SAMs functionalized Au-NPs/GCE. A well-defined peak can be clearly observed at $E = +0.53$ V in all curves, corresponding to the reoxidation of Hg(0) on the SAM surfaces. This result indicates Hg(II) in solution can also incorporate with NH_2 terminal groups of AET SAM. Interestingly, introduction of AET into PET SAM makes the value of $i_{\text{Hg}0}$ rapidly increases to $1.85 \mu\text{A}$, though, this term recorded for SAMs of AET and PET are 0.35 and $1.06 \mu\text{A}$, respectively. The exceeding value of $i_{\text{Hg}0}$ is much over to that obtained by PET-SAM, about 85%. This result is due to not only the presence of NH_2 terminal groups but also a contribution of effects caused by introduction of AET.

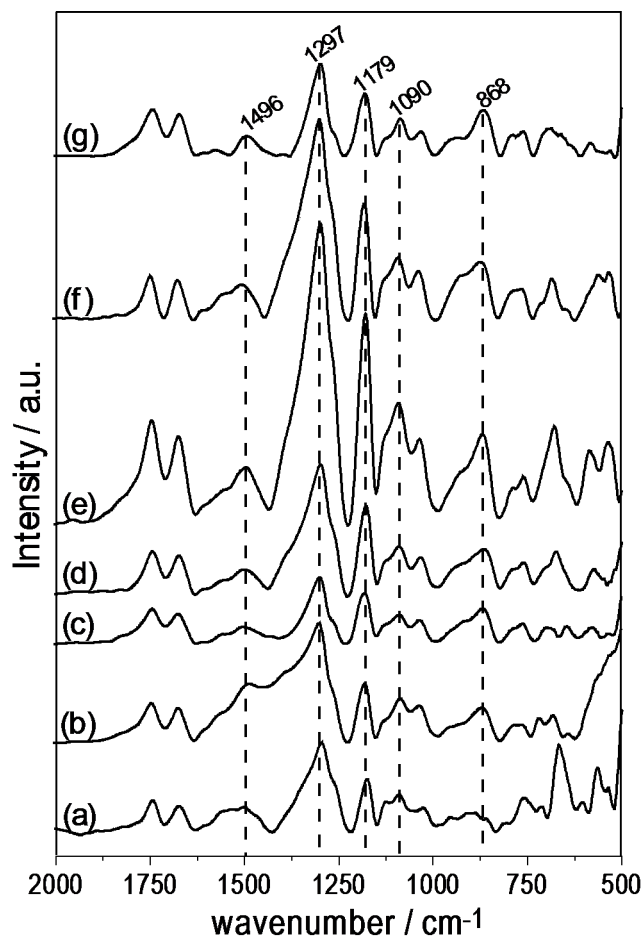


Figure 3. FTIR spectra of SAMs: AET (a); PET (b); and PET-AET-SAMs prepared by immersing PET-SAM into 1.0×10^{-4} M solution of AET for different time: 1 min. (c); 10 min. (d); 20 min. (e); 30 min. (f); and 60 min. (g).

To have a closer look on these effects, we examined kinetic formation of PET-AET SAMs by FTIR technique. For this purpose, the concentration of AET in solution was selected at 1.0×10^{-3} M to investigate immersion time (t_{immer}). In fact, this concentration was selected from investigations of AET concentration dependence of $i_{\text{Hg}0}$ as discussed in the section below. Fig. 3 shows FTIR spectra of different SAMs with most prominently visible bands corresponding assignments based on literatures [30-33]. Briefly, bands at 868, 1090, 1179, 1297, and 1496 cm^{-1} are assigned to (C-H) wagging, CH_2 wagging + (C-C)_{ring} bending, CH_2 wagging + (C-H)_{ring} deformation, (C-H)_{ring} deformation + (C-N) stretching, and (C-C)_{ring} + (C-H)_{ring} deformation. In spectra, extremely weak bands ascribed to CH_2 stretching vibrations in high frequency region are not shown. As seen in curves (a,b) recorded for SAMs of PET and AET SAM, respectively, a similarity in bands except a slightly higher band intensity at 1297 cm^{-1} is observed. This is likely due to the surface of NH_2 little more perpendicular than that of pyridine ring with respect to the surface. When introducing AET into the PET SAM with various t_{immer} , from 1 min. to 20 min., the increase of intensities is visible in curves (c-e). Of those, the bands at 1297

and 1179 cm^{-1} more rapidly raise. This is due to the fact that, initially, when PET SAM is immersed in solution of AET, molecules transfer to the electrode surface and adsorb on vacant sites on Au-NPs, followed by a change their orientation from lying-down phase to standing-up phase for stabilization [34-36]. This process makes the surface of alkyl chain become more perpendicular to the surface. However, only a change in orientation of alkyl chain that is not able to result in such rapid increase of intensities because the spectra of SAMs of PET and AET prepared over night show much lower intensities, as seen curves (a, b). Furthermore, prolongation of t_{immer} increases density of methylene groups in the binary SAMs, but this is not a reason for raising such bands, which rather depends on the dipole moment of bonds in molecules. Therefore, we argued that the significant increase of intensities was a predominant contribution from conformation of pyridine ring.

However, further prolongation of t_{immer} induces a trend of decrease in the intensities as shown in curves (f,g). We elucidated that this phenomenon is time dependence of intermolecular interactions between functional terminal groups in the nearest neighbor molecules in the binary SAMs. This is because these intermolecular interactions easily occur when molecules achieved standing-up phase. Herein, AET is not strongly surface-active due to short alkyl chain length [37], it, thus, needs time to approach to this phase for stabilization [38]. Reinforce for this process is not only van der Waals interactions but also intermolecular interactions between NH_2 terminal group and adjacent N-pyridine to form hydrogen bonding: (AET) $\text{HN-H}\dots\text{N}$ (pyridine). In which AET and PET can act as proton donor and proton acceptor, respectively. The formation of such hydrogen bonding is relative to delocalization in π -electron system of the ring, strengthening (C-H) as well as (C-N). This consequence leads to the decrease of intensities in infra-red spectra, as presented in literatures [39-41].

Thus, introduction of AET to the original PET SAM can be described as following: AET transfer from the bulk solution near the PET-SAM surface to vacant sites on Au-NPs for adsorption. This process can easily take place because of length 1.1 \AA per methylene unit [42,43] accommodating to the distance between the centers of two neighboring pyridine rings, from 3.89 to 4.72 \AA [44,45]. Following, the orientation of AET molecules for stability triggers lateral PET molecules, leading to conformation of pyridine ring at bonds of C-C and C-N [46], and followed by hydrogen bonding formation after a while.

Since those effects are consequences of kinetic processes, we, thus, study influences of t_{immer} on the sensitivity of Hg(II) detection. As seen in Fig. 4, the variation of i_{Hg0} can be divided into three time regions: increase of i_{Hg0} for first ten minutes from the value of $1.0\text{ }\mu\text{A}$, followed by a plateau at the value of $1.8\text{ }\mu\text{A}$ in next about 10 minutes, and after that the value tends lowering. This variation indicates that the incorporation of Hg(II) with terminal groups of the binary SAMs affected by processes in the formation of binary SAMs. The initial duration is essential to stabilize AET molecules adsorbed on vacant sites. This duration is consistent with that reported for complete adsorption of alkanethiols on gold surface from 10 -100 min [47]. Hence, Hg(II) will mainly incorporate with pyridine terminal in preconcentration step. When t_{immer} is sufficiently long time, approximately 10 to 20 minutes, AET can approach stability in binary SAMs. Hg(II) , thus, can incorporate with both NH_2 and pyridine terminal groups possessed the conformation,

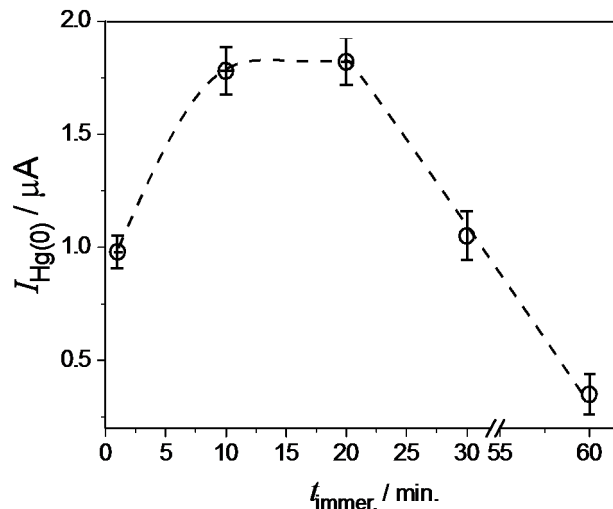


Figure 4. Dependence of peak current of Hg(0) on immersion time. PET-AET SAMs was prepared by AET solution at $1.0 \times 10^{-4}\text{ M}$.

leading to the increase of i_{Hg0} . However, more prolongation of t_{immer} causes the formation of intermolecular hydrogen bonding, that can reduce the incorporation with Hg(II) . This is due to the formation of hydrogen bonds leading to reducing electronegativity in N-atom in pyridine ring. In addition, a sufficiently long time makes AET molecules can also form hydrogen bonding on the SAMs surface with PET molecules existing in clusters, preventing incorporation with Hg(II) in preconcentration step. Such formation of hydrogen bonding on the surface of binary SAM is similar with supramolecular interactions reported by other authors [49,50]. Hence, the variation of i_{Hg0} is consistent with results obtained by FTIR technique.

As argued, the conformation in PET-AET SAM plays the role in enhancing the value of i_{Hg0} . Hence, for the binary SAM, i_{Hg0} should be affected by concentration of AET in solution. This is because adsorption on the surface of molecules depends on their concentration in solution [48]. To prove this argument, we examined variation of i_{Hg0} at various concentrations of AET as shown in Fig. 5a. As seen, there are two distinct regions of i_{Hg0} : a plateau in low concentrations, followed by a decrease of i_{Hg0} in high concentrations. This evidence clearly indicates that the conformation of molecules in the binary SAMs is affected by number AET molecules introduced from solution. Although in the low concentrations, the number of AET molecules is still sufficient to adsorb onto vacant sites on Au-NPs and trigger the adjacent PET molecules to result in conformation. In the higher concentrations, the number AET molecules transfer to the surface become abundant compared with that adsorb on vacant sites. The exceeding AET molecules, thus, are able to form hydrogen bonding on the SAMs surface. Hence, the decrease of i_{Hg0} by increasing concentration of AET is similar with increasing immersion time in this solution. This argument was also examined by FTIR as shown in Fig. 5b. As seen, the intensity of bands also tends to decrease with increasing the concentration of AET. This trend is similar with that when increasing immersion time in AET solution of $1.0 \times 10^{-4}\text{ M}$ over 30 minutes.

Application capability of PET-AET SAMs to determination of

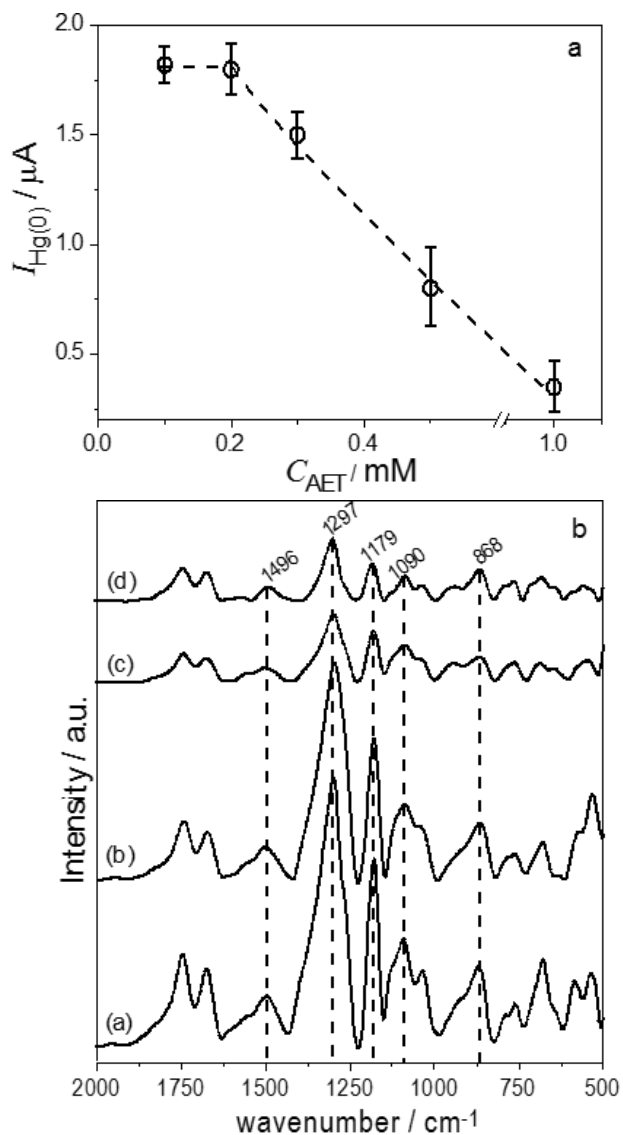


Figure 5. a. Dependence of peak current of Hg(0) on concentration of AET in solution, b. FTIR spectra of PET-AET SAM prepared by immersion of PET SAM for 10 min. in various concentrations of AET in solution: 1.0×10^{-4} M (a); 3.0×10^{-4} M (b); 5.0×10^{-4} M (c); 1.0×10^{-3} M (d).

Hg(II) is depicted in Fig. 6. It is noted that, in order to evaluate the sensitivity of the binary SAMs, we just focused on low concentrations, $\leq 4.97 \times 10^{-9}$ M Hg(II). In this range, the linear dependence of i_{Hg0} on the concentrations of Hg(II) in solution is wider than that obtained for PET SAM. The binary SAM, hence, gives the detection limit estimated from three times the standard deviation of the back ground noise ($s/n = 3$) of 3.85×10^{-12} M, which is approximately three times lower than that given by PET SAM. RSD varied in the range of 1.3 – 4.8 % ($n = 3$). The linear relations between i_{Hg0} and concentration of Hg(II) in solution is depicted by equations shown in the figure, indicating application capability in analysis of Hg(II).

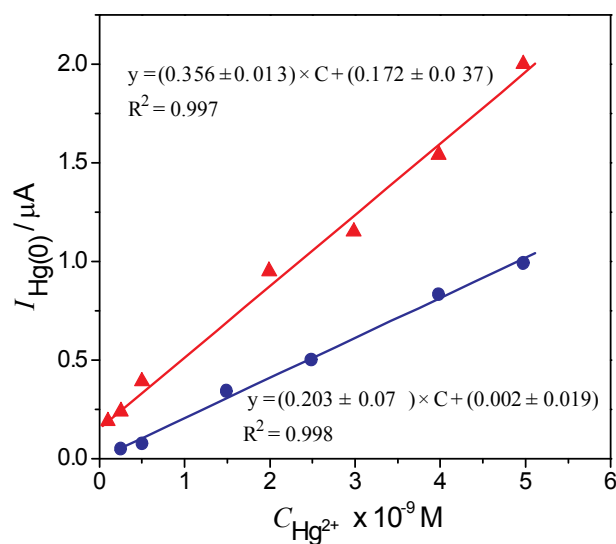


Figure 6. Calibration curves for determination of Hg(II) of SAMs: PET(●); PET-AET (▲).

4. CONCLUSIONS

In our contribution, introduction of AET from solution into the origin PET SAM to form binary PET-AET SAMs for enhancing the sensitivity of Hg(II) detection has been investigated. It has been found that immersion in low concentrations of AET for short time leads to significantly improve the reoxidation peak current of Hg(0). Whereas, immersion in high concentrations of AET for longer time induces the decrease of this peak current. Since results obtained by FTIR, we have elucidated that these effects correspond to conformation of pyridine ring and hydrogen bonding between PET and AET molecules. Obtained results can bring closer look on effects of introducing the second component into the original SAM by adsorption method, as well as their capability in electrochemical analysis of Hg(II).

5. ACKNOWLEDGEMENT

This work was supported by Grant-in-Aid for projects belong to the sections of science and technologies in priority of Viet Nam Academy of Science and Technology (VAST 07.03/13-14).

REFERENCES

- [1] I. Willner, A. Riklin, *Anal. Chem.*, 66, 1535 (1994).
- [2] S.E. Creager, K.G. Olsen, *Anal. Chim. Acta* 307, 277 (1995).
- [3] S.K. Jung, G.S. Wilson, *Anal. Chem.*, 68, 591 (1996).
- [4] E. Chow, D.B. Hibbert, J.J. Gooding, *Analyst*, 130, 831 (2005).
- [5] A. Ulman, *An Introduction to Ultrathin Organic Films. From Langmuir-Blodgett to Self-Assembly*, Academic Press: Boston, 1991.
- [6] A. Ulman, *Chem. Rev.*, 96, 1533 (1996).
- [7] W. Yang, J.J. Gooding, D.B. Hibbert, *J. Electroanal. Chem.*, 516, 10 (2001).
- [8] R.S. Freire, L.T. Kubota, *Electrochim. Acta*, 49, 3795 (2004).
- [9] A. Mohadesi, M.A. Taher, *Talanta*, 72, 95 (2007).

- [10] E. Malel, J.K. Sinha, I. Zawisza, G. Wittstock, D. Mandler, *Electrochim. Acta*, 53, 6753 (2008).
- [11] N. Daud, N.A. Yusof, T.W. Tee, *Int. J. Electrochem. Sci.*, 6, 2798 (2011).
- [12] W. Yang, E. Chow, G.D. Willett, D.B. Hibbert and J.J. Gooding, *Analyst*, 128, 712 (2003).
- [13] R.K. Shervedani, S.A. Mozaffari, *Anal. Chem.*, 78, 4957 (2006).
- [14] E. Chow, D.B. Hibbert, J.J. Gooding, *Analyst*, 130, 831 (2005).
- [15] R. Shabani, S.A. Mozaffari, S.W. Husain, M.S. Tehrani, *Iranian J. Sci. Tech., Transection A*, 33, 335 (2009).
- [16] S. Huan, C.Jiao, Q. Shen, J. Jiang, G.ming Zeng, G.he Huang, G.li Shen, R.Q Yu, *Electrochim. Acta*, 49, 4273 (2004).
- [17] M. Brust, P.M. Blass, A.J. Bard, *Langmuir* 13, 5602 (1997).
- [18] X.-C. Fu, X. Chen, Z. Guo, L.-T. Kong, J. Wang, J.-H. Liu, X.-J. Huang, *Electrochim. Acta*, 56, 463 (2010).
- [19] C.S. Oh, H. Kim, S. Rengaraj, Y. Kim, *Microporous and Mesoporous Materials*, 147, 1 (2012).
- [20] L. Rubinstein, S. Steinberg, Y. Tor, A. Shanzer, J. Sagiv, *Nature*, 332, 426 (1998).
- [21] B. Zeng, X. Ding, F. Zhao, *Electroanalysis*, 14, 651 (2002).
- [22] D. Han, Y.-R. Kim, J.-W. Oh, T.H. Kim, R.K. Mahajan, J.S. Kim, H. Kim, *Analyst*, 134, 1857 (2009).
- [23] P.H. Phong, N.H. Anh, L.Q. Hung, N.T.C Ha, V.T.T. Ha, *Asian. J. Chem.*, 25, 6562 (2013).
- [24] H.-G. Hong, W. Park, E. Yu, *J. Electroanal. Chem.*, 476, 177 (1999).
- [25] T. Komura, T. Yamaguchi, H. Shimatani, R. Okushio, *Electrochim. Acta*, 49, 597 (2004).
- [26] T. Kakiuchi, H. Usui, D. Hobara, M. Yamamoto, *Langmuir*, 18, 5231 (2002).
- [27] S. Imabayashi, M. Iida, D. Hobara, Z.Q. Feng, K. Niki, T. Kakiuchi, *J. Electroanal. Chem.*, 428, 33 (1997).
- [28] C.A. Widrig, C. Chung, M.D. Porter, *J. Electroanal. Chem.*, 310, 335 (1991).
- [29] J.J. Calvente, Z. Kováčová, M.D. Sanchez, R. Andreu, W.R. Fawcett, *Langmuir*, 12, 5696 (23) (1996).
- [30] K. Rajalingam, L. Hallmann, T. Strunskus, A. Bashir, C. Wöll, F. Tuzcek, *Phys. Chem. Chem. Phys.*, 12, 4390 (2010).
- [31] X. Stammer, K. Tonigold, A. Bashir, D. Käfer, O. Shekhah, C. Hülsbusch, M. Kind, A. Groß, C. Wöll, *Phys. Chem. Chem. Phys.*, 12, 6445 (2010).
- [32] M. Robert, G.C. Basseler, C.T. Morrill, *Spectrometric Identification of Organic Compounds*, Jhon Wiley and Sons, Singapore 1981.
- [33] G. Varsanyi, *Vibrational Spectra of Benzen derivatives*, Akademiai Kiado, Budapest, 1969.
- [34] G.E. Poirier, E.D. Pylant, *Science*, 272, 1145 (1996).
- [35] O. Dannenberger, M. Buck, M. Grunze, *J. Phys. Chem. B.*, 103, 2202 (1999).
- [36] D. Qu, M. Morin, *J. Electroanal. Chem.*, 565, 235 (2004).
- [37] L.H. Dubois, R.G. Nuzzo, *Annu. Rev. Chem.*, 43, 437 (1992).
- [38] W. Pan, C.J. Durning, N.J. Turro, *Langmuir*, 12, 4469 (1996).
- [39] J. Joseph, E.D. Jemmis, *J. Am. Chem. Soc.*, 129, 4620 (2007).
- [40] P. Hobza, V. Spirko, H.L. Selzle, E.W. Schlag, *J. Phys. Chem. A* 102, 2501 (1998).
- [41] W. Zierkiewicz, B.C. Matuszewicz, D. Michalska, *J. Phys. Chem. A*, 115, 11362 (2011).
- [42] V.B. Engelkes, J.M. Beebe, C.D. Frisbie, *J. Am. Chem. Soc.*, 126, 14287 (2004).
- [43] X.D. Cui et al, *J. Phys. Chem. B*, 106, 8609 (2002).
- [44] P.C.R. Guillory, J.E. Kirsch, H.K. Izumi, C.L. Stern, K.R. Poeppelmeier, *Crystal Growth & Design*, 6, 382 (2006).
- [45] L.R. Dinelli, G.V. Poelhsitz, E.E. Castellano, J. Ellena, S.E. Galembeck, A.A. Batista, *Inorg. Chem.*, 48, 4692 (2009).
- [46] A. De Binis, G. Compagnini, R.S. Cataliotti, G. Marletta, *J. Raman Spectrosc* 30, 1067 (1999).
- [47] K. Shimazu, I. Wag, Y. Sato, K. Uosaki, *Langmuir* 8, 1385 (1992).
- [48] G.M. Credo, A.K. Boal, K. Das, T.H. Galow, V.M. Rotello, D.L. Feldheim, C.B. Gorman, *J. Am. Chem. Soc.* 124, 9036 (2002).
- [49] T.B. Norsten, E. Jeoung, R.J. Thibault, V.M. Rotello, *Langmuir* 19, 7089 (2003).
- [50] K. Hu, A.J. Bard, *Langmuir*, 14, 4790 (1998).